A TRIANGULAR THICK SHELL FINITE ELEMENT FOR THE THREE-DIMENSIONAL STRESS ANALYSIS OF PRESSURE VESSELS

D.T. RAMANI

Nuclear Power Generation, Babcock-Brown Boveri Reaktor GmbH, D-6800 Mannheim, Germany

SUMMARY

A finite-element method of analysis, based on an exact elasticity solution, including transverse shearing deformation capability is developed herein for the application to the bending of plates and shells of any arbitrary configuration. The field equations of Reissner's thick-plate theory, which includes the effects of transverse shearing deformation have been utilized as guidelines in developing a triangular thick shell flat element for a three-dimensional stress analysis.

The formulation of an orthotropic element, having six nodal points (3 each at top and bottom), has been modeled herein on the basis of trilinear displacement functions, illustrated by equation (1b). The element dealt with herein possesses 36 degrees of freedom (3 rotations and 3 displacements at each node) which represent both membrane and bending (including shearing) deformations. Whereas shearing deformation is coupled with the bending mode, the membrane behavior is considered independent of bending and shearing for simplicity of computations. The procedure for including the shear effects is somewhat similar to other known elements, however, with some fundamental differences, such as the retention of all the components of the strain tensor, $\{\varepsilon\}^e$, for the stiffness matrix generation and treatment of proper boundary conditions along an edge.

The method, presented herein, is consistent with Reissner's assumption of linear bending stress distribution and considers the nodal displacements at the top and bottom, in a bending mode, to vary linearly over the thickness of the plate. However, the transverse displacement does not vary over the thickness of the plate. Further simplification in the development of stiffness matrix occurs, when the bending mode is assumed to be simulated by an anti-symmetric deformation of top and bottom sets of nodes in the element about its middle plane and transverse displacement, is assumed identical at all the nodes.

The preceding considerations and assumptions of Reissner's theory lead to the following displacement functions:

Membrane Mode: $u_m = (\alpha_1 + \alpha_2 x \times \alpha_3 y),\ v_m = (\alpha_4 + \alpha_5 x + \alpha_6 y)$ (1a)

Bending + Shearing Mode:
$$u_b = (\alpha_7 + \alpha_8 x + \alpha_9 y) z$$
$$v_b = (\alpha_{10} + \alpha_{11} x + \alpha_{12} y) z \quad (1b)$$
$$w = (\alpha_{13} + \alpha_{14} x + \alpha_{15} y)$$

The strain vector may be expressed as

$$\{\varepsilon\}^e = \{\varepsilon_{xx}, \varepsilon_{yy}, \varepsilon_{zz}, \varepsilon_{xy}, \varepsilon_{yz}, \varepsilon_{zx}\} \quad (2)$$

Using potential energy formulation, a 6×6 membrane element stiffness matrix, $(K_m)^e$, and a 9×9 bending (including shearing) stiffness matrix, $(K_b)^e$, are generated independently and super-imposed linearly to yield a 15×15 matrix, which then is expanded to an 18×18 stiffness matrix, $(K_b)^e$, to include three fictitious twisting totations $\{\theta_z\}^e$ (at the top or bottom nodes). The corresponding nodal displacement vector may be expressed as

$$\{\delta_l\}^e = \{u_l, v_l, w_l, \theta_x^l, \theta_y^l, \theta_z^l\}^e,\ l = i, j, k. \quad (3)$$

To test the validity of the proposed analysis, results are compared with those of the Reissner theory and other example problems in plates and shells. An excellent agreement in displacements and tractions was obtained. Of particular interest is the ability of the finite-element analysis, based entirely on a displacement formulation, to satisfy the edge conditions and to accurately represent the distribution of shear stress results along an edge.

I. Introduction

The finite element method of analysis is one of the most significant developments of the last decade, in the field of numerical techniques, for the solution of many complex problems of continuum mechanics. The method is based upon applying a Galerkin-Rayleigh-Ritz type solution with piecewise continuous functions expressing the undetermined parameters in terms of nodal quantities. Once this idea was applied to plane stress-plane strain problems, its extension to plate bending and shells was a logical step.

The literature is quite extensive on this subject, and it would be prohibitive to give a detailed discussion of it here. However, it is relevant to discuss briefly three important aspects of the general problem of shell analysis, namely, the basic problem of selecting the appropriate finite element model, the computational problem of obtaining a practical and simplified solution for producing analysis results that can be conveniently used for design purposes, preference of two-dimensional elements to three-dimensional counterparts for complex analyses and, finally, economic limitations on the cost of analytical solution. Such economic limitations are of paramount importance, particularly in three-dimensional analysis, and, at least at the present time, one may not be justified in employing complex finite element models when, for a similar subdivision, simpler elements with fewer number of degrees of freedom and less computational effort can be gainfully utilized.

The increasing use of moderately thick plates and shells in nuclear industry has necessitated systematic and efficient numerical methods of analysis, particularly in dealing with structural deformations that include substantial transverse shearing strains as pointed out by Reissner [1,2] and many other authors.

In the present development, attention is therefore given to many aspects of the three-dimensional problem by using lower-order polynomial representation of both the membrane as well as transverse bending of a plate element, and by developing an economical method of solution. This results in the development of finite element models that can be applied to general three-dimensional shell structures, such as pressure vessels and nozzle-vessel intersections.

II. Behavior of Finite Element Models

A general description of flat triangular elements is furnished by Argyris [3], and arbitrary shells have been successfully studied with flat triangular elements by Clough and Johnson [4], Zienkiewicz [5], Key and Beisinger [6], Oden and Wempner [7], and others. Essentially, the behavior of plates and shells in general has been based on Kirchhoff-hypothesis. The compatibility requirements for bending displacements of Kirchhoff plates and shells are indeed difficult to satisfy, since the interelement continuity must be maintained for the transverse displacement $w(x,y)$ and its derivatives w,x and w,y.

In the analysis of plates and shells, effects of shearing deformation on the bending behavior, both by classical theory as well as finite element methods, have been considered by numerous authors [8 through 22]. Both flat and curved finite element models [23] have been considered and the solution results have been encouraging. However, Kirchhoff-hypothesis for a compatible element either complicates the stiffness formulation or introduces a large number of degrees of freedom.

In the present development of finite element formulation, Reissner's [1] approach is sought after to supplement the existing techniques of including shearing deformations. The method uses the exact elasticity solutions and the field equations of Reissner's widely accepted thick-plate theory have been utilized as guidelines in developing a flat triangular shell element for three-dimensional stress analysis.

III. Field Equations

The modified governing field equations of Reissner's [1] theory for the bending of homogeneous, orthotropic plates, represent the following expressions for the average rotations $\phi_x(x,y)$ and $\phi_y(x,y)$ of cross-sections x=constant and y=constant, respectively.

$$\left.\begin{aligned} \phi_x(x,y) &= \left[\frac{\partial w}{\partial x} - \kappa_1 \left(\frac{Q_{xz}}{G_{xz}h} \right) \right]_{x\,=\,\text{constant}} \\ \phi_y(x,y) &= \left[\frac{\partial w}{\partial y} - \kappa_2 \left(\frac{Q_{yz}}{G_{yz}h} \right) \right]_{y\,=\,\text{constant}} \end{aligned}\right\} \qquad (1)$$

in which κ_1 and κ_2 are numerical shear deflection factors, and where "Gxz" and "Gyz" are shear modulii of an orthotropic element along x=constant and y=constant, respectively. The above equations indicate that straight lines originally normal to the middle surface remain straight but not normal to the deformed middle surface. The above equations may also be expressed as

$$\left.\begin{aligned} \phi_x(x,y) &= \left[\frac{\partial w}{\partial x} + \kappa_1\gamma_{xz}(x,y) \right]_{x\,=\,\text{constant}} \\ \phi_y(x,y) &= \left[\frac{\partial w}{\partial y} + \kappa_2\gamma_{yz}(x,y) \right]_{y\,=\,\text{constant}} \end{aligned}\right\} \qquad (2)$$

Referring to Figs. 1(a),(b) and 6, and assuming linear deformed configuration of the original normal line, one can represent three displacements, u, v, and w, within a continuum by the following expressions

$$\left.\begin{aligned} u(x,y,z) &= z\left[\frac{\partial w}{\partial x} + \kappa_1\gamma_{xz}(x,y) \right] \\ v(x,y,z) &= z\left[\frac{\partial w}{\partial y} + \kappa_2\gamma_{yz}(x,y) \right] \\ w(x,y,z) &= w(x,y) \end{aligned}\right\} \qquad (3)$$

which, in view of Eqns. 1 and 2, may be written as

$$\left.\begin{aligned} u &= z\phi_x(x,y) \\ v &= z\phi_y(x,y) \\ w &= w(x,y) \end{aligned}\right\} \qquad (4)$$

where:

$$\left.\begin{aligned} \phi_x &= \left[\frac{\partial w}{\partial x} + \kappa_1\gamma_{xz} \right] \\ \phi_y &= \left[\frac{\partial w}{\partial y} + \kappa_2\gamma_{yz} \right. \end{aligned}\right\} \qquad (5)$$

The preceding equations are based on the assumptions that total rotations $\phi_x(x,y)$ and $\phi_y(x,y)$ are small and that the transverse strain, $\epsilon_{zz} = \frac{\partial w}{\partial z}$, is negligible. Using three-dimensional equations of elasticity and in view of Eqn. (4), strain-displacement relations may be expressed as

$$\left.\begin{aligned} \epsilon_{xx} &= \frac{\partial u}{\partial x} = z\left(\frac{\partial^2 w}{\partial x^2} + \kappa_1 \frac{\partial \gamma_{xz}}{\partial x} \right) = z\left(\frac{\partial \phi_x}{\partial x} \right) \\ \epsilon_{yy} &= \frac{\partial v}{\partial y} = z\left(\frac{\partial^2 w}{\partial y^2} + \kappa_2 \frac{\partial \gamma_{xz}}{\partial y} \right) = z\left(\frac{\partial \phi_y}{\partial y} \right) \end{aligned}\right\} \qquad (6)$$

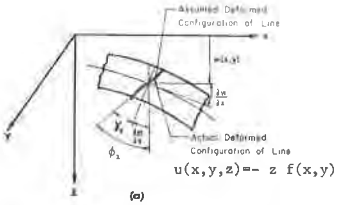

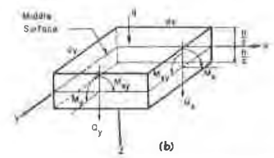

FIG. 1 – DEFINITION OF ASSUMED DEFORMATION STATE FOR SECTION x = CONSTANT

FIG. 1 – STRESS RESULTANTS ON DIFFERENTIAL PLATE ELEMENT

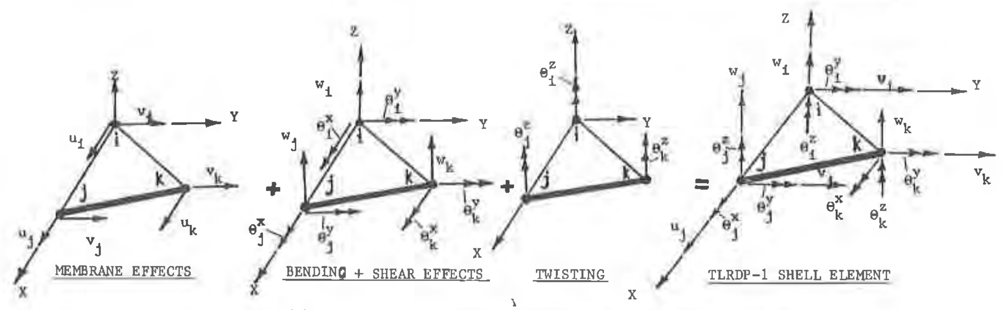

FIG.2(a)-DEVELOPMENT OF TLRDP-1 TRIANGULAR SHELL ELEMENT

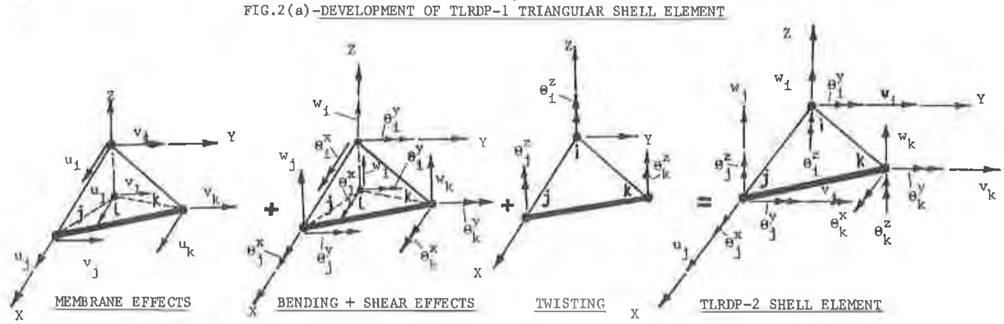

FIG.2(b)- DEVELOPMENT OF TLRDP-2 TRIANGULAR SHELL ELEMENT

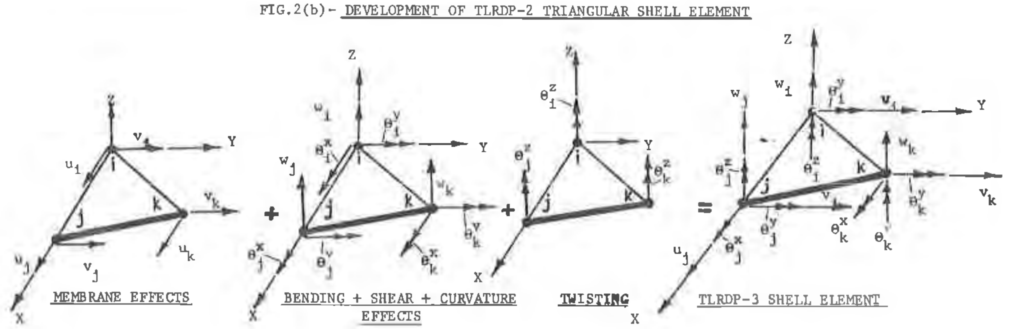

FIG.2(c)- DEVELOPMENT OF TLRDP-3 TRIANGULAR ELEMENT

$$
\left.\begin{aligned}
\varepsilon_{zz} &= \frac{\partial w}{\partial z} = 0 \\
\varepsilon_{xy} &= \left(\frac{\partial u}{\partial y} + \frac{\partial v}{\partial x} \right) = z\left(\frac{\partial \phi_x}{\partial y} + \frac{\partial \phi_y}{\partial x} \right) \\
\varepsilon_{xz} &= \left(\frac{\partial w}{\partial x} + \frac{\partial u}{\partial z} \right) = \kappa_1\left(\frac{\partial w}{\partial x} + \phi_x \right) \\
\varepsilon_{yz} &= \left(\frac{\partial w}{\partial y} + \frac{\partial v}{\partial z} \right) = \kappa_2\left(\frac{\partial w}{\partial y} + \phi_x \right)
\end{aligned}\right\} \qquad (6)\ \text{Cont'd}
$$

Similarly, stress-rotation relations for an orthotropic element may be expressed as

$$
\left.\begin{aligned}
\sigma_x &= \frac{E_x z}{(1 - \nu_x \nu_y)} \left(\frac{\partial \phi_x}{\partial x} + \nu_y \frac{\partial \phi_y}{\partial y} \right) \\
\sigma_y &= \frac{E_y z}{(1 - \nu_x \nu_y)} \left(\frac{\partial \phi_y}{\partial y} + \nu_x \frac{\partial \phi_x}{\partial x} \right) \\
\tau_{xy} &= G_{xy} z \left(\frac{\partial \phi_x}{\partial y} + \frac{\partial \phi_y}{\partial x} \right)
\end{aligned}\right\} \qquad (7)
$$

where:

$$
\left.\begin{aligned}
G_{xy} &= \frac{E_x + E_y}{E_x + E_y(1 + 2\nu_{xy})} \\
\nu_{xy} E_y &= \nu_{yx} E_y
\end{aligned}\right\} \qquad (8)
$$

As customary in moderately thick plates or shells, it is reasonable to assume that effects of normal stress, σ_z, be neglected in this development. This will therefore enable one to compute the shear stresses, τ_{xz} and τ_{yz}, from the following stress equilibrium equations [9], with body forces neglected. Thus,

$$
\frac{\partial \tau_{xz}}{\partial z} = -\left(\frac{\partial \sigma_x}{\partial x} + \frac{\partial \tau_{xy}}{\partial y} \right); \quad \frac{\partial \tau_{yz}}{\partial z} = -\left(\frac{\partial \sigma_y}{\partial y} + \frac{\partial \tau_{xy}}{\partial x} \right) \qquad (9)
$$

which, in view of Eqns. (1) and (7), will yield, upon integration with respect to z, the following expressions:

$$
\left.\begin{aligned}
\tau_{xz} = -\frac{z^2}{2} \Big[& \frac{E_x}{(1-\nu_x\nu_y)} \Big\{ \Big(\frac{\partial^3 w}{\partial x^3} + \kappa_1 \frac{\partial^2 \gamma_x}{\partial x^2} \Big) + \nu_y \Big(\frac{\partial^3 w}{\partial x \partial y^2} + \kappa_2 \frac{\partial^2 \gamma_y}{\partial x \partial y} \Big) \Big\} + G_{xy} \Big(2 \frac{\partial^3 w}{\partial x \partial y^2} \\
& + \kappa_1 \frac{\partial^2 \gamma_x}{\partial y^2} + \kappa_2 \frac{\partial^2 \gamma_y}{\partial x \partial y} \Big) \Big] + g_1(x,y) \\
\tau_{yz} = -\frac{z^2}{2} \Big[& \frac{E_y}{(1-\nu_x\nu_y)} \Big\{ \Big(\frac{\partial^3 w}{\partial y^3} + \kappa_2 \frac{\partial^2 \gamma_y}{\partial y^2} \Big) + \nu_x \Big(\frac{\partial^3 w}{\partial x^2 \partial y} + \kappa_1 \frac{\partial^2 \gamma_x}{\partial x \partial y} \Big) \Big\} + G_{xy} \Big(2 \frac{\partial^3 w}{\partial x^2 \partial y} \\
& + \kappa_1 \frac{\partial^2 \gamma_x}{\partial x \partial y} + \kappa_2 \frac{\partial^2 \gamma_y}{\partial x^2} \Big) \Big] + g_2(x,y)
\end{aligned}\right\} \qquad (10)
$$

in which g_1 and g_2 are integration constants evaluated from the boundary condition that τ_{xz} and τ_{yz} vanish at $z = \pm h/2$. The moment-stress resultants, as illustrated in Fig. 1(b), can now be evaluated in the usual manner by integrating over thickness of the plate to yield

$$
\begin{aligned}
M_x &= -D_x\left(\frac{\partial^2 w}{\partial x^2} + \nu_y \frac{\partial^2 w}{\partial y^2} + \frac{\partial \gamma_x}{\partial x} + \nu_y \frac{\partial \gamma_y}{\partial y} \right) = -D_x\left(\frac{\partial \phi_x}{\partial x} + \nu_y \frac{\partial \phi_y}{\partial y} \right) \\
M_y &= -D_y\left(\frac{\partial^2 w}{\partial y^2} + \nu_x \frac{\partial^2 w}{\partial x^2} + \frac{\partial \gamma_y}{\partial y} + \nu_x \frac{\partial \gamma_x}{\partial x} \right) = -D_y\left(\frac{\partial \phi_y}{\partial y} + \nu_x \frac{\partial \phi_x}{\partial x} \right)
\end{aligned} \qquad (11)
$$

$$M_{xy} = -D_{xy}\left(\frac{2\partial^2 w}{\partial x\partial y} + \frac{\partial\gamma_x}{\partial y} + \frac{\partial\gamma_y}{\partial x}\right) = -D_{xy}\left(\frac{\partial\phi_x}{\partial y} + \frac{\partial\phi_y}{\partial x}\right) \qquad (11)\ \text{Cont'd}$$

where orthotropic constants Dx, Dy, D_{xy}, ν_x and ν_y are defined in Appendix-II. Also using equilibrium equations from Ref. [9], it may be shown that the shear stress-resultants, Q_{xz} and Q_{yz}, can be easily evaluated and may be expressed as

$$\left.\begin{aligned} Q_{xz} &= \frac{\partial}{\partial x}\left[D_x\left(\frac{\partial^2 w}{\partial x^2} + \frac{\partial\gamma_x}{\partial x}\right) + H_{xy}\left(\frac{\partial^2 w}{\partial y^2} + \frac{\partial\gamma_y}{\partial y}\right)\right] \\ Q_{yz} &= \frac{\partial}{\partial y}\left[D_y\left(\frac{\partial^2 w}{\partial y^2} + \frac{\partial\gamma_y}{\partial y}\right) + H_{yx}\left(\frac{\partial^2 w}{\partial x^2} + \frac{\partial\gamma_x}{\partial x}\right)\right] \end{aligned}\right\} \qquad (12)$$

which may be simplified as

$$Q_{xz} = -\frac{\partial}{\partial x}\left(D_x\frac{\partial\phi_x}{\partial x} + H_{xy}\frac{\partial\phi_y}{\partial y}\right); \quad Q_{yz} = -\frac{\partial}{\partial y}\left(D_y\frac{\partial\phi_y}{\partial y} + H_{xy}\frac{\partial\phi_x}{\partial x}\right) \qquad (13)$$

The constants, H_{xy} and H_{yx}, may be given as

$$H_{xy} = H_{yx} = (D_x\nu_y + 2D_{xy}) \qquad (14)$$

The preceding equations are different from analogous equations of classical orthotropic plate theory, as the effects of transverse shear are included in the plate curvatures. In order to show similarity of the foregoing expressions to the corresponding equations of Reissner's theory, the following additional equilibrium equation for a uniformly distributed normal load, q, acting on the element, will be considered:

$$\left[\frac{\partial Q_{xz}}{\partial x} + \frac{\partial Q_{yz}}{\partial y} + q(x,y)\right] = 0 \qquad (15)$$

Employing the relations $Q_{xz} = -\frac{1}{\kappa_1}G_{xz}h\gamma_{xz}$ and $Q_{xz} = -\frac{1}{\kappa_2}G_{yz}h\gamma_{yz}$, substituting them in Eqn. (11), and making use of Eqn. (15), will yield the following expressions of stress-resultants:

$$\begin{aligned} M_x &= -D_x\left(\frac{\partial^2 w}{\partial x^2} + \nu_y\frac{\partial^2 w}{\partial y^2}\right) + \frac{\kappa_1 h^2\{E_y(1+\nu_x) - \nu_y E_x(1+\nu_y)\}}{6E_y(1-\nu_x\nu_y)}\frac{\partial Q_{xz}}{\partial x} - \frac{\nu_x\kappa_1 h^2 E_x(1+\nu_y)q}{6E_y(1-\nu_x\nu_y)} \\ M_y &= -D_y\left(\frac{\partial^2 w}{\partial y^2} + \nu_x\frac{\partial^2 w}{\partial x^2}\right) + \frac{\kappa_2 h^2\{E_x(1+\nu_y) - \nu_x E_y(1+\nu_x)\}}{6E_x(1-\nu_x\nu_y)}\frac{\partial Q_{yz}}{\partial y} - \frac{\nu_y\kappa_2 h^2 E_y(1-\nu_x)q}{6E_x(1-\nu_x\nu_y)} \qquad (16) \\ M_{xy} &= -D_{xy}\left(\frac{2\partial^2 w}{\partial x\partial y}\right) + \frac{\kappa_1 h^2\{E_y(1+\nu_x) - \nu_y E_x(1+\nu_y)\}}{6E_y(1-\nu_x\nu_y)}\frac{\partial Q_{xz}}{\partial x} - \frac{\kappa_2 h^2\{E_x(1+\nu_y) - \nu_x E_y(1+\nu_x)\}}{6E_x(1-\nu_x\nu_y)}\frac{\partial Q_{yz}}{\partial y} \end{aligned}$$

The preceding equations, for the case of a constant distributed load, are similar to those of Reissner theory [1] for an isotropic thick plate in which effects of normal stress, σ_z, have been neglected.

IV. Finite Element Formulation

IV.1 Development of Displacement Models

Solution to the fundamental equations of the Reissner theory, which were presented in the previous section, can be conveniently obtained by using a finite-element displacement formulation. The method presented herein is consistent with Reissner's assumptions of linear bending stress distribution in the element and considers nodal displacements at the top and bottom faces, in bending mode (i.e., anti-symmetric deformation about middle plane) to vary linearly over the thickness of element as shown in Figs. 4, 6, and 7. However, the nodal transverse displacement is independent of the thickness of the plate and may be assumed to be a function of in-plane coordinates x and y only.

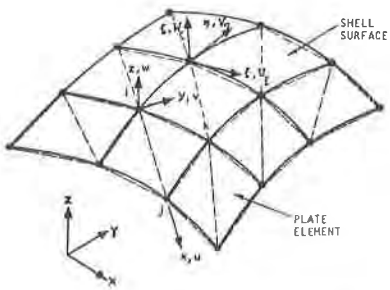

FIG. 3–FINITE-ELEMENT IDEALIZATION OF A SHELL SURFACE

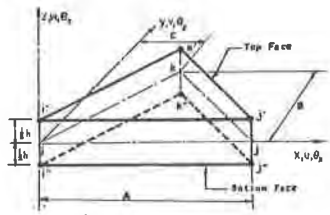

6-NODE MODEL

FIG. 4– TLRDP-1 FINITE ELEMENT FOR SHELL ANALYSIS

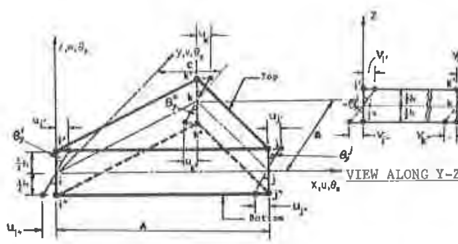

FIG.6– BENDING DEFORMATION MODES OF TLRDP-1 ELEMENT

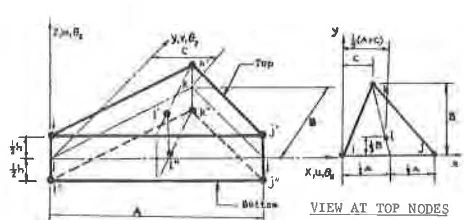

8-NODE MODEL

FIG.5–TLRDP-2 FINITE ELEMENT FOR SHELL ANALYSIS

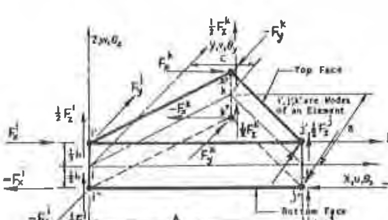

BENDING MODE

FIG. 7–NODAL FORCES ACTING ON TLRDP-1 ELEMENT

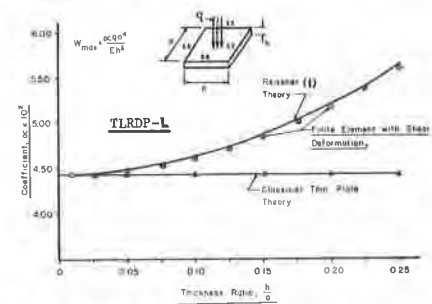

FIG. 8 –INFLUENCE OF TRANSVERSE SHEAR ON MAXIMUM DEFLECTION OF SIMPLY SUPPORTED SQUARE PLATES UNDER UNIFORM LOAD

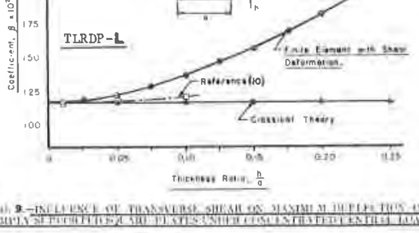

FIG. 9.–INFLUENCE OF TRANSVERSE SHEAR ON MAXIMUM DEFLECTION OF SIMPLY SUPPORTED SQUARE PLATES UNDER CONCENTRATED CENTRAL LOAD

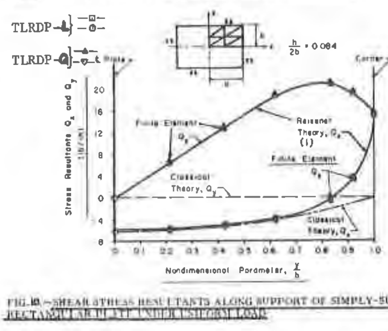

FIG. 10.–SHEAR STRESS RESULTANTS ALONG SUPPORT OF SIMPLY-SUPPORTED RECTANGULAR PLATE UNDER UNIFORM LOAD

The preceding considerations and fundamental assumptions of Reissner's theory lead to the following displacement functions for the bending mode of the triangular element. In developing shell element stiffness matrix, $[K]^e$, the membrane and bending deformations are assumed to be uncoupled. However, in TLRDP-3 element, which is similar to TLRDP-1 and TLRDP-2, additional curvature effects [24] based on shallow shelf theory [14,25] are incorporated.

(a) TLRDP-L Element

This element, designated as Tri-LineaR Displacement Plate Linear model (or briefly TLRDP-L), is a flat plate triangular element and shown typically in Fig. 4. It is incorporated with a five-degree-of-freedom nodal point system. The displacement functions within the element's continuum, may be expressed as

$$\left.\begin{array}{ll} \underline{\text{Bending Mode}} & u_b = (\alpha_1+\alpha_2x+\alpha_3y)z; \quad v_b = (\alpha_4+\alpha_5x+\alpha_6y)z; \quad w_b = (\alpha_7+\alpha_8x+\alpha_9y) \\ \underline{\text{Shearing Mode}} & \gamma_x = (\alpha_{10}+\alpha_{11}x+\alpha_{12}y); \quad \gamma_y = (\alpha_{13}+\alpha_{14}x+\alpha_{15}y) \end{array}\right\} \quad (17)$$

where u_b, v_b, w_b, γ_x and γ_y are defined in Appendix-II. These functions may be conveniently evaluated at the top and bottom nodes and the development of bending stiffness matrix, $[K_b]^e$, which is 15x15, is shown in the following section. The TLRDP-L shell element stiffness may be obtained by static condensation of γ_x and γ_y at the element level into a 9x9 matrix, which is then systematically combined with a 6x6 membrane stiffness matrix, $[K_m]^e$, available in the literature [26].

(b) TLRDP-Q Element

The TLRDP-Q element, illustrated typically in Fig. 5, is a flat plate element and developed also specifically for the analysis of thick plates. This element, unlike TLRDP-L model, possesses 4 nodal points each at the top and bottom faces and a displacement field for bending and shearing deformations within its continuum may be expressed as

$$\underline{\text{Bending Mode}} \quad u_b = (\alpha_1+\alpha_2x+\alpha_3y+\alpha_4xy)z; \; v_b = (\alpha_5+\alpha_6x+\alpha_7y+\alpha_8xy)z; \; w_b = (\alpha_9+\alpha_{10}x+\alpha_{11}y+\alpha_{12}xy)$$

$$\underline{\text{Shearing Mode}} \quad \gamma_x(\alpha_{13}+\alpha_{14}x+\alpha_{15}y+\alpha_{16}xy); \quad \gamma_y = (\alpha_{17}+\alpha_{18}x+\alpha_{19}y+\alpha_{20}xy) \quad (18)$$

The bending stiffness matrix, $[K_b]^e$, which is 20x20, may be easily reduced to 15x15 by means of static condensation at the inner nodes. Similarly, TLRDP-Q shell element may be easily obtained by further static condensation (elimination of γ_x and γ_y) to yield a 9x9 bending stiffness matrix, which can be readily combined with a 6x6 membrane stiffness matrix, $[K_m]^e$.

(c) TLRDP-1 Element

The TLDRP-1 model, based on tri-linear deformations, consists of a flat plate shell element, which is obtained from the following uncoupled membrane and bending displacement functions within the continuum:

$$\underline{\text{Membrane Mode}} \quad u_m = (\alpha_1+\alpha_2x+\alpha_3y); \quad v_m = (\alpha_4+\alpha_5x+\alpha_6y) \quad (19)$$

$$\underline{\text{Bending \& Shearing Mode}} \quad u_b = (\alpha_7+\alpha_8x+\alpha_9y)z; \; v_b = (\alpha_{10}+\alpha_{11}x+\alpha_{12}y)z; \; w_b=(\alpha_{13}+\alpha_{14}x+\alpha_{15}y) \quad (20)$$

in which membrane and bending displacement terms have been defined earlier. The shearing strains, ε_{xz} and ε_{yz}, are incorporated in the element strain vector $\{\varepsilon\}^e$ in developing bending stiffness matrix, $[K_b]^e$. However, these strain components are suppressed as independent degrees of freedom, γ_x and γ_y, in the above displacement functions. This element, which is shown in Figs. 2 and 4, consists of 3 nodes each at the top and bottom faces, and only an upper half of the triangular prism is needed to develop [21] a bending stiffness matrix,

$[K_b]^e$, by means of an anti-symmetric deformation. The membrane stiffness matrix, $[K_m]^e$, may then be directly combined to $[K_b]^e$ to yield a 15x15 shell element stiffness matrix, $[K]^e$, as illustrated in Ref. [27].

(d) TLRDP-2 Shell Element

The TLRDP-2 shell element, which is shown in Figs. 2(b) and 5, has been modelled to include "xy" terms in the displacement functions. The element, which has 4 nodes each at the top and bottom faces, possesses following displacement functions for uncoupled membrane and bending deformation states:

Membrane Mode $\quad u_m = (\alpha_1+\alpha_2x+\alpha_3y+\alpha_4xy);\quad v_m = (\alpha_5+\alpha_6x+\alpha_7y+\alpha_8xy) \qquad (21)$

Bending & Shearing Mode
$$\left.\begin{aligned} u_b &= (\alpha_9+\alpha_{10}x+\alpha_{11}y+\alpha_{12}xy)z;\quad v_b = (\alpha_{13}+\alpha_{14}x+\alpha_{15}y+\alpha_{16}xy)z \\ w_b &= (\alpha_{17}+\alpha_{18}x+\alpha_{19}y+\alpha_{20}xy) \end{aligned}\right\} \qquad (22)$$

in which the shearing strains, ε_{xz} and ε_{yz}, are incorporated in the strain vector $\{\varepsilon\}^e$. The sub-elemental approach (16) of static condensation is adopted to develop an overall element membrane and bending stiffness matrices, $[K_m]^e$ and $[K_b]^e$, respectively. $[K_m]^e$ is a 6x6 matrix and $[K_b]^e$ is a 9x9 matrix. They may be systematically combined to yield a 15x15 shell element stiffness matrix, $[K]^e$, as outlined in Ref. [21].

(e) TLRDP-3 Shell Element

The TLRDP-3 element is similar to TLRDP-1 element except curvature effects are incorporated into the former. This element is essentially modelled on the basis of shallow shell theory [14] and method of including curvature effects into its stiffness matrix is outlined in reference [17]. To obtain an overall shell element stiffness matrix (See Fig. 2(c)), additional curvature stiffness terms are added on to the bending stiffness matrix, $[K_b]^e$, which is then linearly combined with membrane stiffness matrix, $[K_m]^e$, as discussed earlier.

IV.2 Assembled System Stiffness and Method of Analysis

The method of analysis consists in idealizing (Fig. 3) an arbitrary plate or shell structure by a network of flat plate triangular elements. Each element is isolated and its stiffness and load matrices are then derived [5] based on foregoing assumed admissable deformation patterns. In the present case, the membrane stiffness, $[K_m]^e$, and the bending stiffness, $[K_b]^e$, are uncoupled and one way to minimize interlement incompatibility is to express the membrane and bending displacements in terms of like polynomial functions of the same order as has been done in the present analysis.

The three-dimensional method of analysis used herein is a direct extension of two-dimensional analysis including transverse shearing deformation. A brief description of the procedure is given here. Once the displacement field, $\{f_\alpha\}^e$, is specified, the element stiffness, $[K_\alpha]^e$, can be easily obtained by the procedure outlined in Ref. [5]. The result is a nodal force-displacement relationship, for a typical finite element, of the following form;

$$\{F\}^e = [K]^e\ \{\delta\}^e \qquad (23)$$

or, more explicitly,

$$\begin{Bmatrix} \{F_m\}^e \\ \{F_b\}^e \\ \{F_\theta\}^e \end{Bmatrix} = \begin{bmatrix} [K_m]^e & [0] & [0] \\ [0] & [K_b]^e & [0] \\ [0] & [0] & [0] \end{bmatrix} \begin{Bmatrix} \{\delta_m\}^e \\ \{\delta_b\}^e \\ \{\delta_\theta\}^e \end{Bmatrix} \qquad (24)$$

where $\{F_m\}^e$, $[K_m]^e$ and $\{\delta_m\}^e$ refer to the membrane force vector, stiffness matrix and displacement vector, respectively. The bending quantities $\{F_b\}^e$, $[K_b]^e$ and $\{\delta_b\}^e$ are similarly identified. The twisting quantities $\{F_\theta\}^e$ and $\{\delta_\theta\}^e$ correspond to ficticious nodal torque and rotation vectors, respectively [5] and are introduced for completeness only. These quantities and corresponding stiffness terms appear as a result of transformation into global system. The nodal displacement vector, $\{\delta_u\}^e = \{u_b^i, v_b^i, w_b^i, \gamma_x^i, \gamma_y^i, \text{etc.}...\}$, evaluated at the top (or bottom) nodes in Fig. 7 from Eqn. (17) may be easily shown to be related to $\{\delta_b\}^e$ as

$$\{\delta_b\}^e = [\Phi_T]^T \{\delta_u\}^e \tag{26}$$

in which $[\Phi_T]$ is a transformation matrix. Similarly, it may be shown that

$$\{F_b\}^e = [\Phi_T] \{F_u\}^e \tag{27}$$

In developing the bending stiffness matrix, $[K_b]^e$, of an element, use has been made of minimization of potential energy which yields

$$[K_b]^e = \int_V [B_b^e]^T [D_b^e][B_b^e]d(\text{Vol}) \tag{28}$$

in which element strain-displacement matrix, $[B_b^e]$, is related to nodal displacement vector $\{\delta_b\}^e$ as

$$\{\varepsilon_b\}^e = [B_b^e]\{\delta_b\}^e \tag{29}$$

where $\{\varepsilon_b\}^e = \{\varepsilon_x, \varepsilon_y, \varepsilon_z, \varepsilon_{xy}, \varepsilon_{yz}, \varepsilon_{zx}\}$, can easily be obtained by using Eqn. (6). Similarly, an orthotropic elasticity matrix, $[D_b^e]$, is obtained from stress-strain relations as

$$\{\sigma_b\}^e = [D_b^e]\{\varepsilon_b\}^e \tag{30}$$

where $\{\sigma_b\}^e = \{\sigma_x, \sigma_y, \sigma_z, \tau_{xy}, \tau_{yz}, \tau_{zx}\}^e$, is a three-dimensional stress vector within a continuum. The equilibrium equations of the overall system are formed by assembling the force-displacement relation, $\{F\}^e = [K]^e\{\delta\}^e$, of each individual element through coordinate transformations from the element (See Fig. 3) coordinate system (x,y,z) to global system (X,Y,Z) and finally into curvilinear coordinate system (ξ, η, ζ). This method is elaborately discussed and adopted in Ref. [21], in which a large capacity computer program, capable of handling three-dimensional shell analysis, is incorporated. The formulation of an overall shell element stiffness matrix from its component deformation states may be expressed as

$$[K]^e = [K_m]^e + [K_b]^e + [K_s]^e + [K_c]^e \tag{31}$$

in which $[K]^e$, $[K_m]^e$, $[K_b]^e$, $[K_s]^e$ and $[K_c]^e$ are element, membrane, bending, shearing, and curvature-effects stiffness matrices, respectively.

V. Numerical Examples

To test the validity of the proposed analysis, a few numerical problems are solved and their solution results are compared with those of Reissner theory and other known exact methods. Due to limitation of space, only a few types of elements are dealt with herein to bring out their effectiveness in analyzing the complex problems. Proper boundary conditions are enforced on the degrees of freedom, incorporated in each model of the proposed method, along each edge.

V.1 Simply-Supported Square Plate With Uniform Load

The first problem analyzed herein consists of an isotropic simply-supported square plate (shown in Fig. 8) subjected to uniform transverse load, q, and discretized with TLRDP-L element using (4x4), (8x8) and (16x16) mesh sizes on a quarter plate. The boundary conditions are taken as

(i) along the edge - $u_b \neq 0$, $v_b = 0$, $w_b = 0$, $\gamma_x \neq 0$, $\gamma_y = 0$ (32)

(ii) along the continuous boundary - $u_b = 0$, $v_b = 0$, $w_b \neq 0$, $\gamma_x = 0$, $\gamma_y = 0$ (33)

The comparison of finite element analysis with Reissner theory, for non-dimensionalized deflection results, is illustrated in Fig. 8, in which the influence of thickness-ratio, h/a, on deflection coefficient,"α", is presented. The comparison of numerical results is seen to be very favorable and there is an excellent agreement.

V.2 Simply-Supported Square Plate With Concentrated Central Load

The second problem presented herein also consists of an isotropic simply-supported square plate subjected to a concentrated central load, P, and discretized with TLRDP-L element, using (4x4), (8x8) and (16x16) mesh sizes on a quarter plate. The boundary conditions prescribed are similar to those in the previous problem. No known solution based on Reissner's theory is available for this problem; however, available finite element solution results [10] compare very favorably with the proposed method. Such a comparison is shown in Fig. 9, which represents the influence of dimensionless parameter, h/a, on deflection coefficient, "β", including shearing effects. As expected, there is a marked increase in deflection due to shear for a corresponding increase in dimensionaless parameter h/a.

V.3 Simply-Supported Rectangular Plate With Uniform Load

The third problem, which consists of an isotropic simply-supported rectangular plate subjected to transverse uniform load, q, was selected to bring out essentially an accurate distribution of shear stress-resultants, Qx, Qy, and Mxy as shown in Fig. 10 and 11. Both TLRDP-L and TLRDP-Q elements were utilized in discretizing a quarter plate, using (4x4), (8x8) and (16x16) mesh sizes. The prescribed boundary conditions are the same as those of previous examples. An excellent agreement between the proposed method and Reissner theory is obtained for the distribution of stress-resultants Qx, Qy, and Mxy, as observed. However, a striking difference between the finite element analysis and classical theory results is found along the supported edge.

V.4 Line-Loaded Long Circular Cylinder

The fourth problem deals with a line-loaded long isotropic Circular Cylinder for which a closed-form solution is available in Ref. [9]. This problem (Fig. 12) was analyzed to predict a response of finite element solution to a three-dimensional analysis, using TLRDP-1, TLRDP-2 and TLRDP-3 elements. Due to symmetry of the problem and bending of local character [9] within a finite length, only a small sliced section (3"xπ/32), was chosen [21] for mesh idealization. Proper boundary conditions were enforced on the sliced section in curvilinear system as follows:

(i) along symmetrical section $\theta=0$ $u_\xi\neq0$, $v_\eta=0$, $w_\zeta\neq0$, $\theta_\xi=0$, $\theta_\eta\neq0$, $\theta_\zeta=0$ (34)

(ii) along the sliced section $\theta=\pi/32$ $u_\xi\neq0$, $v_\eta\neq0$, $w_\zeta\neq0$, $\theta_\xi\neq0$, $\theta_\eta\neq0$, $\theta_\zeta\neq0$ (35)

(iii) along the sliced section x=3" $u_\xi=0$, $v_\eta\neq0$, $w_\zeta\neq0$, $\theta_\xi\neq0$, $\theta_\eta=0$, $\theta_\zeta=0$ (36)

The finite element solution results compare very favorably with those of Ref. [9].

V.5 Nozzle-Cylinder Subjected to Hydrostatic Pressure

The fifth problem, that is of utmost importance in the nuclear industry and analyzed by only a few investigators [28,29], consists of an experimental model of a nozzle-to-cylinder intersection problem, analyzed experimentally at ORNL by [28]. Figure 14 illustrates the model, which is subjected to an internal pressure of 202 psi. Both TLRDP-1 and TLRDP-2 elements were employed in the finite element analysis on the discretized section shown in

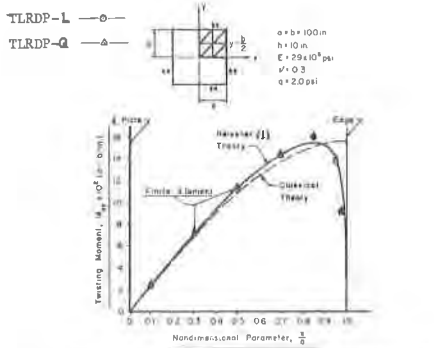

FIG. 11.- DISTRIBUTION OF TWISTING MOMENT ALONG SECTION y = b/2

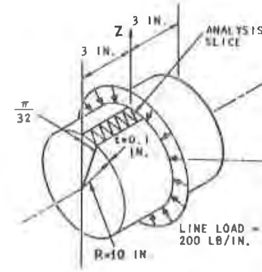

FIG 12-LINE-LOADED CYLINDER

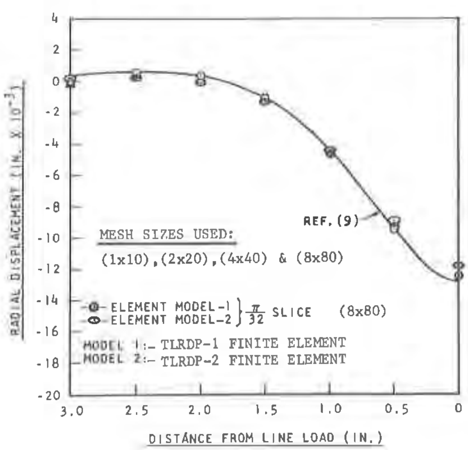

FIG.13- RADIAL DISPLACEMENT FOR LINE-LOADED CYLINDER

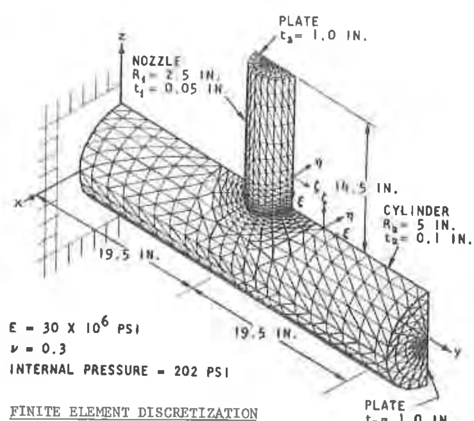

FIG.14-NOZZLE-TO-CYLINDER INTERSECTION

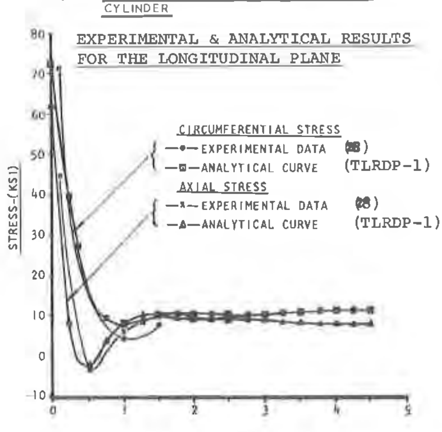

FIG 15 NOZZLE STRESSES

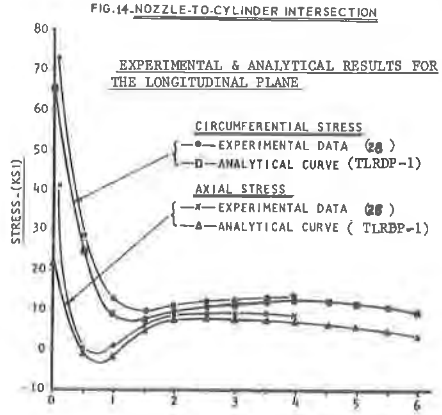

FIG.16 CYLINDER STRESSES

in Fig. 14. Because of extremely large size of problem, modified versions of computer codes "SANSHL" [21] and "SAP" [30] were utilized to include TLRDP-1, TLRDP-2, and TLRDP-3 finite elements in analyzing the chosen problem. It may be observed that finite element results by the proposed method compare very well with the experimental and analytical results of Refs. [28,29]. The analytical results yielded by both TLRDP-1 and TLRDP-2 are found to be very close to each other in this problem. Nozzle and cylinder stresses are shown in Figs. 15 and 16, respectively.

VI. Conclusions

An analytical method, based on finite-element displacement formulation as well as Reissner's theory, is presented here. These triangular finite elements, which include membrane, bending and shearing deformation states, are used for the analyses of several example problems. The proposed method is well-suited for pressure vessel and nozzle-cylinder intersections as well as for a general three-dimensional analysis. The utilization of consistent and compatible displacement fields in membrane, bending and shearing states allows meaningful idealization of three-dimensional structures. The additional transverse shearing degrees of freedom on shearing effects enable one to prescribe the most realistic boundary conditions. It may be concluded that the proposed method as well as formulation offer a convenient and concise method for including transverse shearing effects for the analyses of both two- and three-dimensional problems.

Acknowledgements - The author would like to express his sincere gratitude to Prof. W. Wunderlich of Ruhr-Universität, Bochum, Germany, and Mr. J. M. Anderton of Babcock & Wilcox Company, Lynchburg, Virginia, U.S.A. for their valuable advice and encouragement. The author is also grateful to Mr. H. Krämer and other colleagues of Babcock-Brown Boveri Reaktor GmbH, Mannheim, Germany, for their assistance in computing services.

Appendix I - References

[1] Reissner, E. "The Effect of Transverse Shear Deformation on the Bending of Elastic Plates," Journal of Applied Mechanics, Vol. 12, 1945, pp. 69-77.

[2] Reissner, E. "On Some Problems in Shell Theory," Proc. First Symp. on Naval Structural Mechanics. Pergamon Press, N.Y., 1960.

[3] Argyris, J. H., "Continua and Discontinua," Proc. Conf. on Matrix Methods in Structural Mechanics. Wright-Patterson AFB, Dayton, 1966.

[4] Clough, R. W. and Johnson, C. P., "A Finite Element Approximation for the Analysis of Thin Shells," Internat. Journal of Solids and Structures, Vol. 4, 1968, pp. 43-60.

[5] Zienkiewicz, O. C., The Finite Element Method in Structural and Continuum Mechanics, McGraw-Hill Book Co., New York, 1967.

[6] Key, S. W. and Beisinger, Z., "The Analysis of Thin Shells With Transverse Shear Strains by the Finite Element Method," Proc. of Second Air Force Conf. on Matrix Methods in Struct. Mech., Ohio, 1968.

[7] Oden, J. T. and Wempner, G. A., "Numerical Analysis of Arbitrary Shell Structures Under Arbitrary Static Loading," Tech. Report-47, University of Alabama Research Institute, Huntsville, Nov., 1967.

[8] Love, A. E. H., "A Treatise on the Mathematical Theory of Elasticity," Dover Publ., New York, 4th ed., 1927.

[9] Timoshenko, S. P. and Woinowsky-Krieger, S., Theory of Plates and Shells, McGraw-Hill Book Co., New York, 1959.

[10] Smith, Ian M., "A Finite Element Analysis for 'Moderately Thick' Rectangular Plates in Bending," International Journal of the Mechanical Sciences, Vol. 10, 1968, pp. 563-570.

[11] Carley, T. G. and Langhaar, H. L., "Transverse Shearing Stress in Rectangular Plates," Journal of the Engineering Mechanics Division, ASCE, Vol. 94, No. EM1, Proc. Paper 5795,

Feb., 1968, pp. 137-151.

[12] Green, A. E., "On Reissner's Theory of Bending of Elastic Plates," Quarterly of Applied Mathematics, Vol. 7, 1949.

[13] Salerno, V. L. and Goldberg, M. A., "Effect of Shear Deformation on the Bending of Rectangular Plates," Journal of Applied Mechanics, Vol. 27, 1960.

[14] Marguerre, K., "Zur Theorie der Gekrummenten Platte Grosser Formanderung," Proc. 5th Internat. Congress of Applied Mech., Cambridge, Mass., 1938.

[15] Argyris, J. H. and Scharpf, D., "The SHEBA Family of Shell Elements for the Matrix Displacement Method," Aeronautical Journal, Oct., 1968, Mar., May, 1969.

[16] Clough, R. W. and Felippa, C. A., "A Refined Quadrilateral Element for Analysis of Plate Bending," Proc. II Conf. on Matrix Methods in Structural Mechanics, Wright-Patterson AFB, Ohio, 1968.

[17] Utku, S. and Melosh, R. J., "Behavior of Triangular Shell-Element Stiffness Matrices Associated With Ployhedral Deflection Distributions," AIAA Journal, Vol. 6, No. 2, Feb., 1963.

[18] Anderheggen, E., "Finite Element Plate Bending Equilibrium Analysis," Journal of the Engineering Mechanics Division, ASCE, Vol. 95, No. EM4, Proc. Paper 6715, Aug., 1969, pp. 841-857.

[19] Herrman, L. R., "A Bending Analysis for Plates," Proc. I Conference on Matrix Methods in Structural Mechanics, Wright-Patterson AFB, Ohio, 1967.

[20] Chung, T. J. and Bandy, M. A., "Finite Element Analysis of Thick Shell of Revolution," Journal ASCE EM.4, Paper-1315, Aug., 1971.

[21] Ramani, D. T., "The Finite Element Analysis of Sandwich Buckle-Shell Structures," Doctoral Dissertation, Purdue University, Lafayette, Ind., Jan., 1972.

[22] Pryor, C. W., Barker, R. M., and Frederick, D., "Finite Element Bending Analysis of Reissner Plates," Journal ASCE, EM.6, Dec., 1970.

[23] Dhatt, G., "Numerical Analysis of Thin Shells by Curved Triangular Elements Based on Discrete-Kirchoff Hypothesis," Proc. of Symposium on Application of Finite Element Methods in Civil Engineering, Vanderbilt University, Nov. 13-14, 1969.

[24] Utku, S., "Stiffness Matrices for Thin Triangular Elements of Non-Zero Gaussian Curvature," AIAA Journal, Vol. 5, No. 9, Sept., 1967, pp. 1650-1657.

[25] Pecknold, D. A. W. and Schnobrich, W. C., "Finite Element Analysis of Skewed Shallow Shells," Journal of the Structural Division, ASCE, Vol. 95, ST4, Proc. Paper 6523, Apr., 1969.

[26] Turner, M. J., Clough, R. W., Martin, H. C., and Topp, L. J., "Stiffness and Deflection Analysis of Complex Structures," Journal of the Aeronautical Sciences, Vol. 23, No. 9, Sept., 1956, pp. 805-823.

[27] Meyers, V. J., Ramani, D. T., and Greenwood, M. E., "Plastic Sandwich Buckle-Shell Structures," Journal ASCE, ST11, Paper-9323, Nov., 1972.

[28] Greenstreet, W. L., Moore, S. E., and Callahan, J. P. "Third Annual Progress Report on Studies in Applied Solid Mechanics," Oak Ridge National Laboratory Report No. ORNL-4821, Dec., 1972.

[29] Prince, N. and Rashid, Y. R., "Structural Analysis of Shell Structures' Intersections," First International Conf. on Pressure Vessel Technology, Delft, The Netherlands, Oct., 1969.

[30] Wilson, E. L., "Solid SAP-A Static Analysis Program for Three-Dimensional Solid Structures," University of California Report No. UCSESM 71-19, Sept., 1971.

Appendix II - Notations

The following notations are used in this paper:

A,B,C = dimensions of a finite element

a,b = dimensions of a rectangular plate

$\{B^e\}$ = strain-displacement matrix of an element

$[D^e]$ = constitutive stress-strain relation matrix

D_x, D_y = bending rigidities of an orthotropic plate in x and y directions
D_{xy} = torsional rigidity of an orthotropic plate
e = superscript denoting a finite element
E_x, E_y = modulii of elasticity in x and y directions
$\{f_\alpha\}^e$ = displacement field of a finite element in which α=m (membrane) or α=b (bending).
$\{F\}^e$ = vector of nodal forces for a finite element
$\{F_b\}^e$ = vector of bending nodal forces of an element
$\{F_m\}^e$ = vector of membrane nodal forces of an element
$\{F_u\}^e$ = vector of nodal forces at the top or bottom set of nodes
$\{F_\theta\}^e$ = vector of ficticious twisting nodal forces of an element
$g_1(x,y)$, $g(x,y)$ = integration constants
G_{xz}, G_{yz} = shear modulii of sections x = constant and y = constant
G_{xy} = shear modulus of an orthotropic plate
H_{xy}, H_{yx} = effective torsional rigidities of an orthotropic plate
h = thickness of plate
$[K_b]^e$ = bending stiffness matrix of a finite element in x,y,z system
$[K_m]^e$ = membrane stiffness matrix of an element in x,y,z system
$[K_c]^e$ = curvature stiffness matrix of an element in x,y,z system
$[K]^e$ = an overall finite element stiffness matrix in x,y,z system
M_x, M_y, M_{xy} = moment stress resultants in x,y,z system
[0] = null matrix
P = a concentrated central load
q = transverse uniform distributed load
Q_{xz}, Q_{yz} = transverse shear stress resultants
Q_x, Q_y = transverse shear forces
T = superscript denoting transpose of a matrix
u,v,w = displacements at a point along x,y,z directions
u_b, v_b, w_b = displacements of a point of a finite element along x,y,z directions
u_i, v_i, w_i = generalized displacements at node "i" along x,y,z axes
u_m, v_m = in-plane displacements of a point in x,y system
u_ξ, v_η, w = displacements along ξ, η, ζ axes
x,y,z = local coordinate system of plate element
X,Y,Z = global coordinate system of the structure
$\alpha_1, \alpha_2, \alpha_3 \ldots$ = nodal displacement parameters
α = a dimensionless constant; a subscript
β = a dimensionless constant
γ_x, γ_y = average transverse shear strains along sections x = constant and y = constant
γ_{xz}, γ_{yz} = transverse shear strains of sections x = constant and y = constant
$\{\delta\}^e$ = vector of nodal displacements of an element
$\{\delta_b\}^e$ = vector of bending nodal displacements of an element
$\{\delta_m\}^e$ = vector of membrane nodal displacements of an element
$\{\delta_\theta\}^e$ = vector of twisting nodal displacements of an element
$\{\delta_u\}^e$ = vector of nodal displacements at the top or bottom set of nodes
$\{\varepsilon\}^e$ = strain matrix of a finite element

M 3/

$\{\varepsilon_b\}^e$ =bending strain matrix of an element

$\varepsilon_{xx},\varepsilon_{yy},\varepsilon_{zz},\varepsilon_{xy},\varepsilon_{yz},\varepsilon_{zy}$ = components of the strain tensor in x,y,z system

$\theta_x^i,\theta_y^i,\theta_z^i$ = generalized rotations at node "i" about x,y,z axes

ν_{xy},ν_{yx} = Poisson's ratio of an orthotropic material

ν_x,ν_y = Poisson's ratio in the direction of x and y

κ_1,κ_2 = shear deflection factors along sections x = constant and y = constant

$\{\sigma\}^e$ = stress matrix of a finite element

$\sigma_x,\sigma_y,\sigma_z,\tau_{xy},\tau_{yz},\tau_{zx}$ = components of the stress tensor in x,y,z system

ϕ_x,ϕ_y = total rotation of sections x = constant and y = constant

$\{\Phi_T\}$ = transformation matrix

ξ,η,ζ = curvilinear coordinate system of the surface